

# INSOLATION CHANGES ON PLUTO CAUSED BY ORBITAL ELEMENT VARIATIONS

E. VAN HEMELRIJCK

*Belgian Institute for Space Aeronomy, Brussels, Belgium*

(Received 10 September, 1984)

**Abstract.** In this paper, we compare changes in the insolation at Pluto, corresponding to three epochs during the dynamical history of the planet:  $t = -1, 0$  and  $0.5$ , where  $t$  is the time in millions of years A.D. The two extreme values of  $t$  coincide respectively with a maximum ( $126^\circ$ ) and a minimum ( $102^\circ$ ) value of the obliquity ( $\epsilon$ ). The other orbital elements i.e. the eccentricity ( $e$ ) and the longitude of the perihelion ( $\lambda_p$ ) which affect solar radiation and which are apt to significant periodic changes are also calculated for the times under consideration. In a series of figures, the combined influence of the evolving dynamic parameters on the daily insolation and on the mean (summer, winter, annual) daily insolation is illustrated.

## 1. Introduction

Calculations of the daily solar radiation incident at the top of Pluto's atmosphere and its variability with latitude and season were presented by Van Hemelrijck (1982a, b) for three fixed values of the obliquity ( $\epsilon = 60, 75, \text{ and } 90^\circ$ ), cited in the literature, and for the presently adopted values of the eccentricity ( $e$ ) and the longitude of the perihelion ( $\lambda_p$ ). From the two extreme values of the obliquity interval mentioned above it can be seen that, at the time of the publication of the two papers, the angle between the planet's spin axis and its orbit normal was very poorly determined (Davies *et al.*, 1980). The obtained results, however, illustrated fairly well the sensitivity of Pluto's insolation to changes in  $\epsilon$ .

In a paper, recently published by Dobrovolskis and Harris (1983), the authors investigated the history of Pluto's obliquity by numerical integration using analytic approximations of Williams and Benson (1971). They found that the obliquity varies between  $\sim 102^\circ$  and  $\sim 126^\circ$  over a time period of about 3 million years, with a current pole position described by  $\epsilon = 118.5$  (see also Harris and Ward, 1982) implying that Pluto's rotation is slightly retrograde.

In this work, we examine variations in the insolation at Pluto corresponding to three epochs during the dynamical history of the planet. The orbital configurations we have modeled are the cases when  $\epsilon = 102, 118.5, \text{ and } 126^\circ$ . As noted earlier, the values of  $\epsilon$  represent the extreme values of the oscillation cycle ( $102$  and  $126^\circ$ ) and the current one ( $118.5$ ) and are, e.g., reached at approximately  $t = -1, 0.5, \text{ and } 0$  respectively,  $t$  being the time in millions of years A.D. (Dobrovolskis and Harris, 1983). The knowledge of  $t$  is indispensable for the computation of other planetary data, particularly the eccentricity and the longitude of the perihelion.

In a first section we briefly summarize some expressions needed for the determination

of the upper-boundary insolation of the outer planets. Then, taking into account adopted or computed orbital and planetary data of Pluto, we calculated the planetocentric longitude of its perihelion. The results of the daily insolation are presented in the form of three contour maps showing the incident solar radiation in  $\text{cal cm}^{-2} (\text{planetary day})^{-1}$  as a function of latitude and solar longitude and in two figures illustrating the seasonal variation of the equatorial and polar solar energy. In addition, the latitudinal variation of the mean solar radiations are included in a series of three plots.

## 2. Calculation of the Insolation

The daily insolation may be written as (see e.g. Ward, 1974; Vorob'yev and Monin, 1975; Levine *et al.*, 1977; Van Hemelrijck, 1982a, b, c; 1983).

$$I_D = [S_0 T (1 + e \cos W)^2 / \pi a_\odot^2 (1 - e^2)^2] (h_0 \sin \varphi \sin \delta_\odot + \sin h_0 \cos \varphi \cos \delta_\odot), \quad (1)$$

where  $S_0$  is the solar constant at the mean Sun–Earth distance of 1 AU taken at  $1.96 \text{ cal cm}^{-2} (\text{min})^{-1}$  (Wilson, 1982),  $T$  is the sidereal day (6.3867 earth days),  $e$  is the eccentricity,  $a_\odot$  is the semi-major axis (39.45 AU),  $h_0$  is the local hour angle at sunset (or sunrise),  $\varphi$  is the planetocentric latitude,  $\delta_\odot$  is the solar declination and  $W$  is the true anomaly which is given by

$$W = \lambda_\odot - \lambda_p, \quad (2)$$

where  $\lambda_\odot$  and  $\lambda_p$  are respectively the planetocentric longitude of the Sun (called solar longitude in the figures) and the planetocentric longitude of the planet's perihelion.

The parameters  $h_0$  and  $\delta_\odot$  may be obtained from standard spherical trigonometric relationships, whereas Pluto's eccentricity  $e$  may be expressed in the form (Williams and Benson, 1971; Dobrovolskis and Harris, 1983)

$$e = 0.244 + 0.022 \cos \Psi + 0.005 \cos 3\Psi, \quad (3)$$

where  $\psi = 72^\circ.8 + 91^\circ.2 t$  and  $t$  is the time in millions of years A.D.

Furthermore, the mean (summer, winter, annual) daily insolations, hereafter denoted as  $(\bar{I}_D)_S$ ,  $(\bar{I}_D)_W$ , and  $(\bar{I}_D)_A$  respectively, may be found by integrating numerically relation (1) within the appropriate time limits and by dividing the obtained result by the corresponding length of the season ( $T_S$  or  $T_W$ ) or by the tropical year ( $T_0 = 90\,583$  earth days; Golitsyn, 1979). For the calculation of  $T_S$  or  $T_W$  we refer e.g. to Van Hemelrijck (1982b).

## 3. Calculation of the Planetocentric Longitude of the Perihelion

According to the paper of Vorob'yev and Monin (1975), the planetocentric longitude of the perihelion ( $\lambda_p$ ) may be written in terms of the argument of perihelion ( $\omega$ ) as

$$\lambda_p = \omega + \Lambda, \quad (4)$$

where  $\Lambda$  is the planetocentric longitude of the ascending node altered by  $180^\circ$ . A detailed description of the computing algorithm to obtain  $\Lambda$  is beyond the scope of this work. We only mention that it depends upon several orbital and planetary data and can be expressed in the general form (Vorob'yev and Monin, 1975)

$$\Lambda = f(i, \Omega, \tilde{\omega}, \epsilon, \epsilon_0, \alpha_0, \delta_0), \quad (5)$$

with

$$\tilde{\omega} = \Omega + \omega, \quad (6)$$

where  $i$ ,  $\Omega$ ,  $\tilde{\omega}$ ,  $\epsilon$ ,  $\epsilon_0$ ,  $\alpha_0$ , and  $\delta_0$  are, respectively, the inclination to the ecliptic, the mean longitude of the ascending node, the mean longitude of the perihelion, the obliquity, the angle between the Earth's spin axis and its orbit normal ( $\epsilon_0 = 23^\circ.45$ ) and the right ascension and declination of Pluto's north pole.

Finally, with respect to the invariable plane of the solar system,  $i$ ,  $\Omega$ , and  $\omega$  are well represented as (Williams and Benson, 1971; Dobrovolskis and Harris, 1983)

$$i = 15^\circ.91 - 1^\circ.04 \cos \Psi, \quad (7)$$

$$\Omega = 111^\circ.428 - 97^\circ.209t - 1^\circ.5 \sin \Psi, \quad (8)$$

and

$$\omega = 90^\circ.0 + 24^\circ.0 \sin \Psi. \quad (9)$$

For the direction of the north pole, we adopted the recommended values for the equatorial coordinates ( $\alpha_0 = 305^\circ$ ,  $\delta_0 = 5^\circ$ ) recently published by the IAU Working Group on cartographic coordinates and rotational elements of the planets and satellites (Davies *et al.*, 1980). It has to be emphasized that the direction of the axis of rotation varies with time. For Pluto, however, the time dependence of  $\alpha_0$  and  $\delta_0$  being unknown, our computations were made by holding the standard equatorial coordinates constant at values corresponding to the epoch 1950.0.

TABLE I  
Numerical parameters for the computation of the insolation at Pluto.

$t$ (millions of years)	$\epsilon$ ( $^\circ$ )	$e$	$\lambda_p$ ( $^\circ$ )	$T_S$ (earth days)	$T_W$ (earth days)
-1	$\sim 102$	0.2678	252.0	59864	30719
0	118.5	0.2466	191.7	48249	42334
0.5	$\sim 126$	0.2386	138.6	36086	54497

Table I represents, for the three epochs under consideration, the numerical values for the calculation of  $I_D$ ,  $(\bar{I}_D)_S$ ,  $(\bar{I}_D)_W$ , and  $(\bar{I}_D)_A$ . It is instructive to note that  $T_S$  and  $T_W$  represent the lengths of the summer and winter corresponding to the northern hemisphere. For the southern one, the two values have to be interchanged.

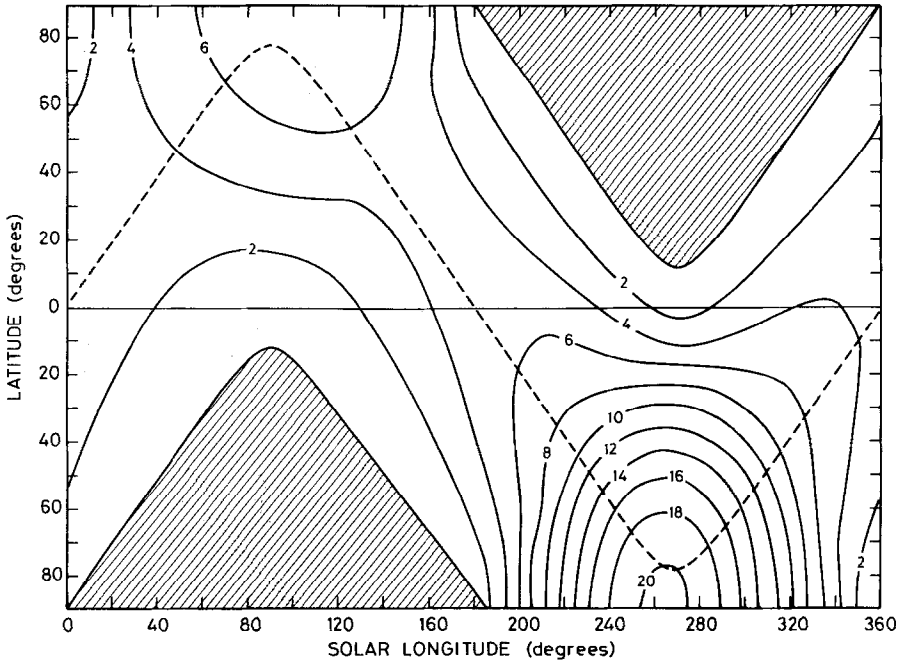


Fig. 1. Seasonal and latitudinal variation of the daily insolation ( $I_D$ ) at the top of the atmosphere of Pluto at the epoch  $t = -1$  ( $\epsilon = 102^\circ$ ,  $e = 0.2678$ ,  $\lambda_p = 252^\circ.0$ ). Solar declination is represented by the dashed line. The areas of permanent darkness are shaded. Values of  $I_D$  in  $\text{cal cm}^{-2}$  (planetary day) $^{-1}$ , are given on each curve.

#### 4. Discussion of Calculations

From expressions (1) and (2), where  $h_0$  and  $\delta_\odot$  are dependent upon  $\epsilon$ , it is obvious that periodic insolation variations are closely associated with changes in the obliquity, the eccentricity and the longitude of perihelion. As already mentioned in the introduction we studied three orbital situations:  $\epsilon = 102^\circ$  ( $t = -1$ ),  $\epsilon = 118.5^\circ$  ( $t = 0$ ) and  $\epsilon = 126^\circ$  ( $t = 0.5$ ) and we determined the corresponding eccentricities and the longitudes of perihelion through expressions (3) to (9). It follows that the calculated insolation regimes are affected by the combined influences of the three orbital elements  $\epsilon$ ,  $e$  and  $\lambda_p$ .

It is important to note that the very large obliquities ( $\epsilon > 90^\circ$ ) of Pluto result in a position reverse of the two hemispheres: the northern hemisphere is 'below' the ecliptic, the southern one 'above' it.

##### 4.1. DAILY INSOLATION

For the daily insolation we have followed the method adopted by e.g. Vorob'yev and Monin (1975), Levine *et al.* (1977) and Brinkman and McGregor (1979) in presenting the results in the form of contour maps showing the seasonal distribution in terms of the

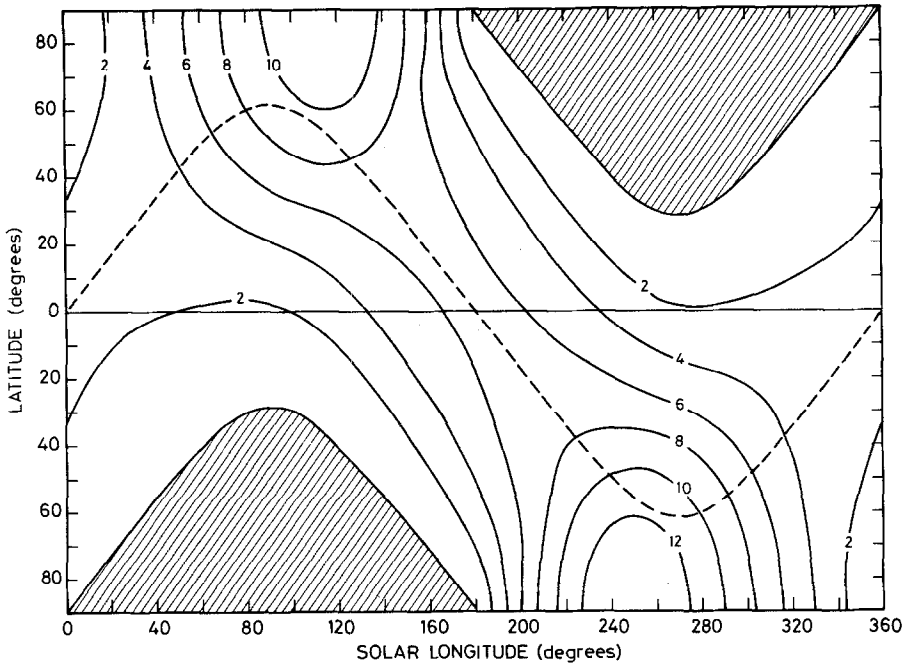


Fig. 2. Seasonal and latitudinal variation of the daily insolation ( $I_D$ ) at the top of the atmosphere of Pluto at the epoch  $t = 0$  ( $\epsilon = 118^\circ.5$ ,  $e = 0.2446$ ,  $\lambda_p = 191^\circ.7$ ). See Figure 1 for full explanation.

planetocentric longitude of the Sun taken to be  $0^\circ$  at the northern hemisphere vernal equinox. Furthermore, we have included two figures giving the latitudinal variation of the daily insolation at the equator and the poles as a function of solar longitude. Application of expression (1) leads to the isopleths illustrated in Figure 1 (1 million years ago), Figure 2 (present situation) and Figure 3 (within 500 000 years) and in Figures 4 and 5. From the contour maps and particularly from Figures 4 and 5 it can be seen that the maximum solar radiation is incident at the poles in the neighborhood of the summer solstices with values of about 7.7 ( $t = -1$ ) to 14.6 ( $t = 0.5$ ) [ $\text{cal cm}^{-2}$  (planetary day) $^{-1}$ ] (north pole) and 8.3 ( $t = 0.5$ ) to as much as 20.7 ( $t = -1$ ) [ $\text{cal cm}^{-2}$  (planetary day) $^{-1}$ ] (south pole). This clearly indicates that the maximum solar radiations, occurring over the poles, experience an approximately twofold increase (or decrease) over a time span of about  $1.5 \times 10^6$  yr. The contour maps, and especially Figure 5, also reveal that the solar radiation at the north pole at summer solstice [ $(I_D)_{NP(ss)}$ ] is smaller than the corresponding solar energy at the south pole [ $(I_D)_{SP(ss)}$ ] for  $\epsilon = 102$  and  $118^\circ.5$  and higher for an obliquity equal to  $126^\circ$ . This can easily be evaluated by computing this insolation at both poles which gives (Van Hemelrijck, 1982b)

$$(I_D)_{NP(ss)} = (S_0 T \sin \epsilon / a_\odot^2) [(1 + e \sin \lambda_p) / (1 - e^2)]^2, \quad (10)$$

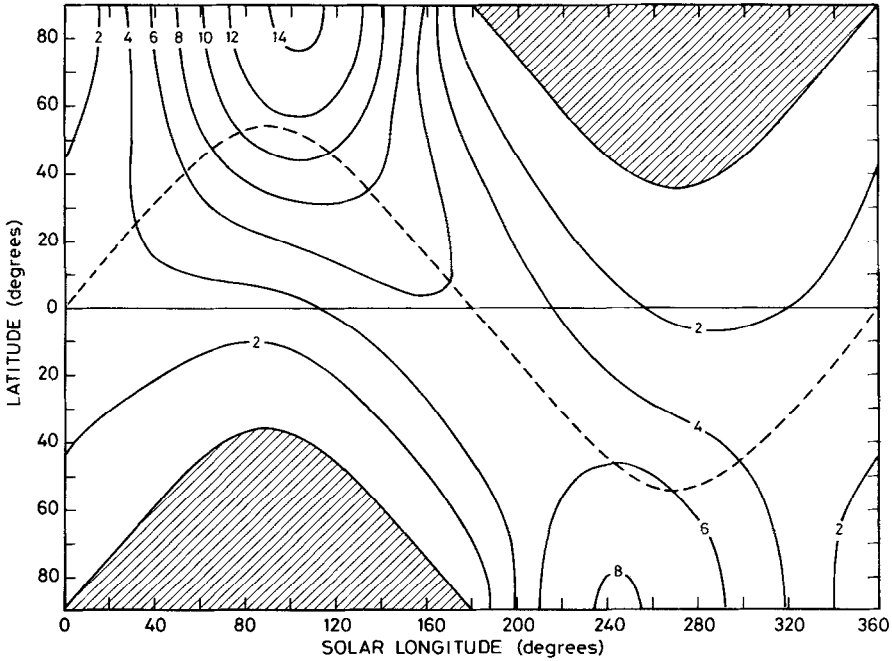


Fig. 3. Seasonal and latitudinal variation of the daily insolation ( $I_D$ ) at the top of the atmosphere of Pluto at the epoch  $t = 0.5$  ( $\epsilon = 126^\circ$ ,  $e = 0.2386$ ,  $\lambda_p = 138.6$ ). See Figure 1 for full explanation.

$$(I_D)_{SP(ss)} = (S_0 T \sin \epsilon / a_\odot^2) [(1 - e \sin \lambda_p) / (1 - e^2)]^2, \quad (11)$$

or

$$(I_D)_{NP(ss)} / (I_D)_{SP(ss)} = [(1 + e \sin \lambda_p) / (1 - e \sin \lambda_p)]^2. \quad (12)$$

Hence:

$$(I_D)_{NP(ss)} > (I_D)_{SP(ss)} \text{ if } 0^\circ < \lambda_p < 180^\circ \quad (t = 0.5)$$

and

$$(I_D)_{NP(ss)} < (I_D)_{SP(ss)} \text{ if } 180^\circ < \lambda_p < 360^\circ \quad (t = -1 \text{ and } t = 0)$$

The equatorial summer solstice insolation, hereafter denoted as  $(I_D)_{E(ss)}$ , may be found from relationship (1) by putting  $\varphi = 0^\circ$ ,  $\lambda_\odot = 90^\circ$  or  $270^\circ$  and  $h_0 = 90^\circ$  and is given by

$$(I_D)_{E(ss)} = (S_0 T \cos \epsilon / \pi a_\odot^2) [(1 \pm e \sin \lambda_p) / (1 - e^2)]^2, \quad (13)$$

where the plus sign is for the northern summer solstice and the minus sign for the southern one.

Dividing (10) or (11) by (13) we obtain the well-known relation

$$(I_D)_{P(ss)} / (I_D)_{E(ss)} = \pi \tan \epsilon, \quad (14)$$

From expression (14) it follows that the ratio of both insulations is larger than unity for  $17.7 < \epsilon < 162.3$  and that it is exclusively dependent upon the obliquity. For  $\epsilon$  equal to 102, 118.5 and  $126^\circ$ , this ratio amounts, respectively, to 14.8, 5.8 and 4.3.

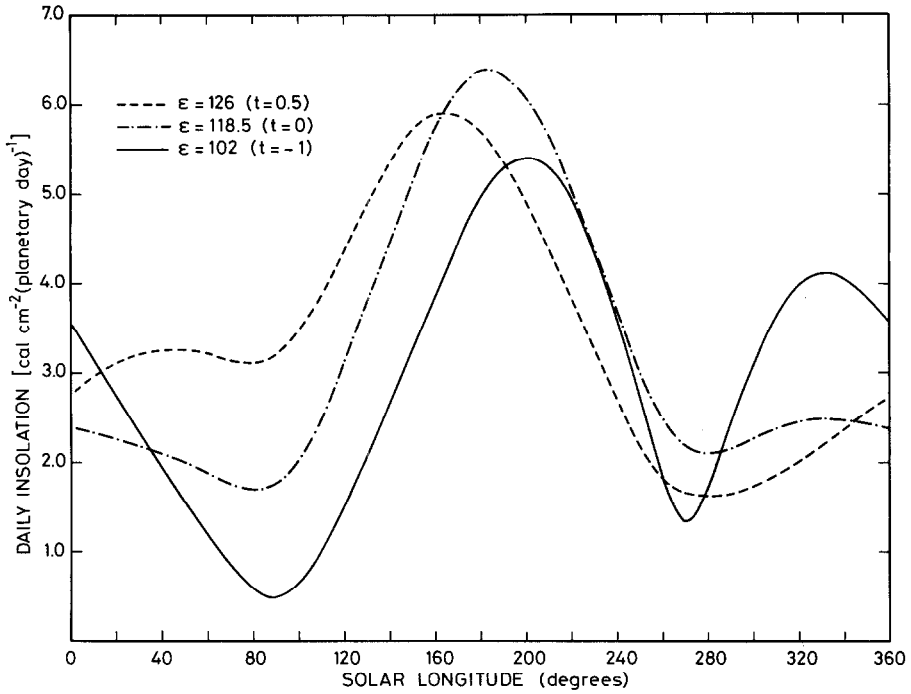


Fig. 4. Seasonal variation of the daily insolation ( $I_D$ ) at the equator of Pluto at  $t = -1$  ( $\epsilon = 102^\circ$ ),  $t = 0$  ( $\epsilon = 118.5^\circ$ ), and  $t = 0.5$  ( $\epsilon = 126^\circ$ ).

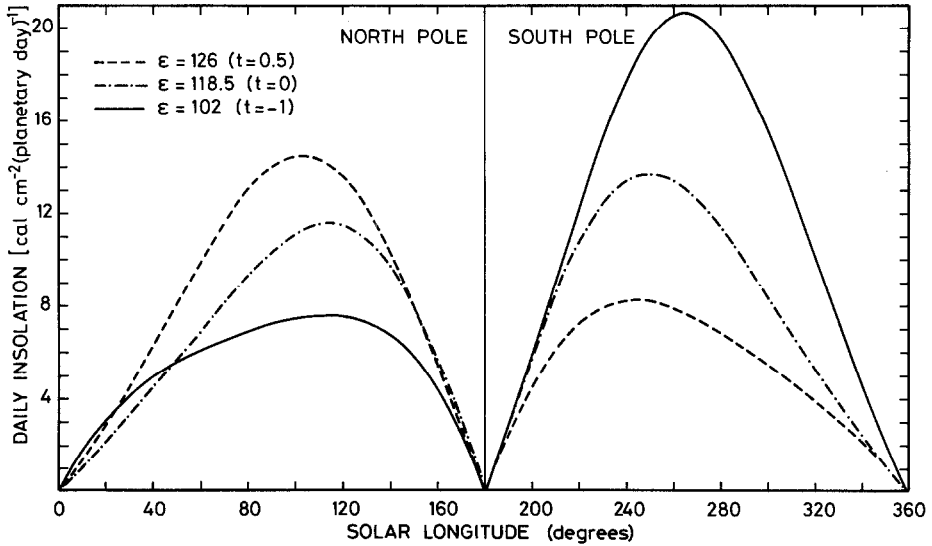


Fig. 5. Seasonal variation of the daily insolation ( $I_D$ ) at the poles of Pluto at  $t = -1$  ( $\epsilon = 102^\circ$ ),  $t = 0$  ( $\epsilon = 118.5^\circ$ ), and  $t = 0.5$  ( $\epsilon = 126^\circ$ ).

From Figures 1 to 3 and Figure 5 it can be seen that the daily insolation at the north pole during summer solstice increases with increasing  $\epsilon$ , whereas at the south pole the opposite effect is found. This conclusion can be derived from expressions (10) and (11), where the obliquity produces variations in the peak insolations through the  $\sin \epsilon$  dependence of the solar flux (first bracket) and whereas the term in the second bracket represents the dependence of  $(I_D)_{NP(ss)}$  or  $(I_D)_{SP(ss)}$  on the eccentricity and the longitude of the perihelion.

First, it has to be emphasized that the value of  $(1 - e^2)^2$  in (10) and (11) changes by only about 3% between the two extremes of the obliquity range. On the other hand, the dependence of the polar energy on  $\sin \epsilon$  and particularly on  $(1 \pm e \sin \lambda_p)^2$  is more sensitive. Indeed, in going from  $\epsilon = 102^\circ$  to  $\epsilon = 126^\circ$ ,  $\sin \epsilon$  depress by about 17%, whereas  $(1 + e \sin \lambda_p)^2$  and  $(1 - e \sin \lambda_p)^2$  increases, respectively decreases, by approximately 141 and 54%. The combined effect of the altering terms is illustrated in Figure 5.

The seasonal variation of the daily insolation at the equator of Pluto for the three values of the obliquity are depicted in Figure 4. According to Figures 4 and 5, the increase of  $(I_D)_{NP(ss)}$  when  $\epsilon$  varies from  $102$  to  $126^\circ$  is accompanied by a corresponding increase of the equatorial solar radiation over practically the entire solar longitude interval ( $0$ – $180^\circ$ ). On the other hand, the loss of the solar energy over the south pole in going from  $102$  to  $126^\circ$  is roughly followed by a decrease of the solar radiation at the equator, particularly in the ( $280$ – $360^\circ$ ) solar longitude range.

More generally, the solar longitude interval where  $(I_D)_P$  exceeds  $(I_D)_E$  can easily be determined from (1) showing that

$$(I_D)_P / (I_D)_E = \pm \pi \tan \delta_\odot = \pm \pi \sin \epsilon \sin \lambda_\odot / (1 - \sin^2 \epsilon \sin^2 \lambda_\odot)^{1/2}, \quad (15)$$

the plus sign being used for the north pole, the minus sign for the southern one. Introducing the numerical values of  $\epsilon$  in Equation (15) we find that, for the north pole,  $(I_D)_P > (I_D)_E$  if  $\lambda_\odot$  ranges from about  $20$  to  $160^\circ$ . For the south pole, the polar daily insolation is greater than that at the equator in the appropriate solar longitude interval ( $200$ – $340^\circ$ ).

The contour maps, and more obviously Figure 5, reveal that the position of maximum solar radiation is shifted, in some cases by nearly  $30^\circ$ , from the position of the summer solstices. The reason for this phenomenon is that the position of the perihelion ( $\lambda_p$ ), varying from about  $140$  to  $250^\circ$ , is located approximately  $130$  to  $20^\circ$  from the south summer solstice. From the plotted curves (Figure 5) it can be seen that the maximum solar radiations occur near  $100$ – $110^\circ$  and  $240$ – $260^\circ$ , depending on the value of the obliquity.

It is well known that a large eccentricity (which is the case for Pluto) produces important north-south seasonal asymmetries in the daily insolation (Figures 1 to 3 and Figure 5). On the other hand, changes in the obliquity causes mainly a global latitudinal redistribution (Figure 4 and 5).

When comparing Figures 1, 2 and 3 it is obvious that, during the dynamical history of Pluto, the insolation pattern may be strongly affected by fluctuations of the orbital elements. Figure 1, representing the daily insolation distribution about one million years ago, shows complete asymmetry between both hemispheres. As an example, the peak insolation at the south pole during summer solstice is nearly three times higher than that of the north pole during its summer solstice. It can also be seen that in the southern hemisphere during summer, the amount of solar radiation very rapidly changes during the course of the year, especially at polar region latitudes.

Figure 2 represents a plot of the current situation of the daily insolation curves. The northern and southern hemispherical distributions are roughly symmetrical. In the solar longitude interval ( $90-270^\circ$ ) and especially at equatorial and mid-latitudes, the isocontours closely parallel the curve representing the seasonal march of the Sun.

North-south differences in the daily insolation are also demonstrated in Figure 3 ( $t = 0.5$ ). However, in contrast with Figure 1 and even with Figure 2,  $(I_D)_{NP(ss)}$  is about two times higher than  $(I_D)_{SP(ss)}$ . As already mentioned earlier, the position of the perihelion [see also expression (12)] is responsible for this enhancement.

Another point of interest concerns the distribution of the daily solar radiation in the equatorial region. For the outer planets and at obliquities smaller than  $45^\circ$ , the latitudinal insolation has one maximum and one minimum if, of course, the polar night is taken as a minimum (Vorob'yev and Monin, 1975; Van Hemelrijck, 1982b). Pluto, and also Uranus, occupies a rather peculiar position in that it rotates lying nearly on its side in its orbital plane. Summer and winter are, roughly speaking, repeated twice a year in the equatorial zone, the two seasons being substantially more temperate than in the polar regions. This characteristic feature is clearly demonstrated in Figure 4 (contrast also this diagram with Figure 5).

#### 4.2. MEAN DAILY INSOLATION

The mean daily insulations, taken over a season or a year, are shown in Figures 6, 7 and 8.

Figure 6, representing the latitudinal variation of the mean summer daily insolation for the three obliquities considered, shows that in the northern hemisphere and at all latitudes,  $(\bar{I}_D)_S$  increases with increasing obliquity ( $\epsilon$ ); in the southern hemisphere the opposite effect is found. For comparison, if  $\epsilon$  varies from  $102$  to  $126^\circ$ ,  $(\bar{I}_D)_S$  in the northern hemisphere changes from  $5.7$  to  $7.7 \text{ cal cm}^{-2} (\text{planetary day})^{-1}$  and from  $1.9$  to  $3.8 \text{ cal cm}^{-2} (\text{planetary day})^{-1}$  at the north pole and the equator respectively. In the southern hemisphere, and when  $\epsilon$  increases from its minimum to its maximum value, the equatorial solar energy declines from  $3.8$  to  $2.5 \text{ cal cm}^{-2} (\text{planetary day})^{-1}$ , whereas the polar insolation drops from  $11.0$  to  $5.1 \text{ cal cm}^{-2} (\text{planetary day})^{-1}$ .

The sensitivity of e.g. the summertime polar insolation to fluctuations in  $\epsilon$ ,  $T_S$  and  $e$  can easily be illustrated by its expression (Murray *et al.*, 1973; Ward, 1974; Vorob'yev and Monin, 1975; Van Hemelrijck, 1982b):

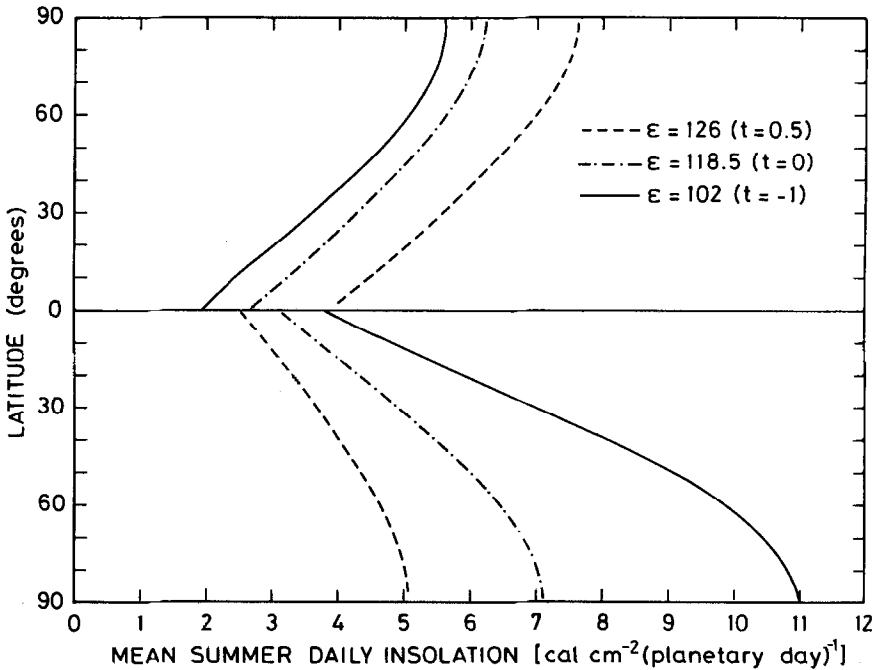


Fig. 6 Latitudinal variation of the mean summer daily insolation  $(\bar{I}_D)_S$  at the top of the atmosphere of Pluto at  $t = -1$  ( $e = 102^\circ$ ),  $t = 0$  ( $e = 118.5$ ), and  $t = 0.5$  ( $e = 126^\circ$ )

$$(\bar{I}_D)_{S_P} = (S_0 T T_0 \sin \epsilon / T_S) / \pi (1 - e^2)^{1/2} a_\odot^2. \quad (16)$$

First, we note that  $(\bar{I}_D)_{S_P}$  is only weakly dependent on  $e$ . As the eccentricity varies from 0.2386 to 0.2678 (Table I), the insolation changes only by about 1%. On the other hand, expression (16) is quite sensitive to variations in both the obliquity and the length of the summer season. By introducing the numerical values of  $\epsilon$  and  $T_S$  (Table I) into (16) it follows that  $(\bar{I}_D)_{S_P}$  is a monotonically increasing function of  $\epsilon$  at the north pole and a monotonically decreasing function at the south pole.

The non-coincidence at the equator of the curves (Figures 6 and 7) representing the northern and southern solar radiation distribution at equal values of the obliquity is owing to the arbitrary chosen definition of the seasons in both hemispheres. In our calculations and for the northern hemisphere, the summer season is defined as running from the vernal equinox over summer solstice to autumnal equinox and spanning  $180^\circ$ ; consequently, the planetocentric longitudes  $\lambda_\odot = 180^\circ$  and  $\lambda_\odot = 360^\circ$  mark the beginning and the end of the winter period. In the southern hemisphere, the solar longitude intervals  $(0 - 180^\circ)$  and  $(180 - 360^\circ)$  divide the year into astronomical winter and summer respectively.

The mean winter daily insulations corresponding to the three obliquities are plotted in Figure 7. Since in winter the Sun does not rise at the poles, it is obvious that  $(\bar{I}_D)_{W_P} = 0$ . At all latitudes, the effect of increasing obliquity causes the insolation to reduce in the

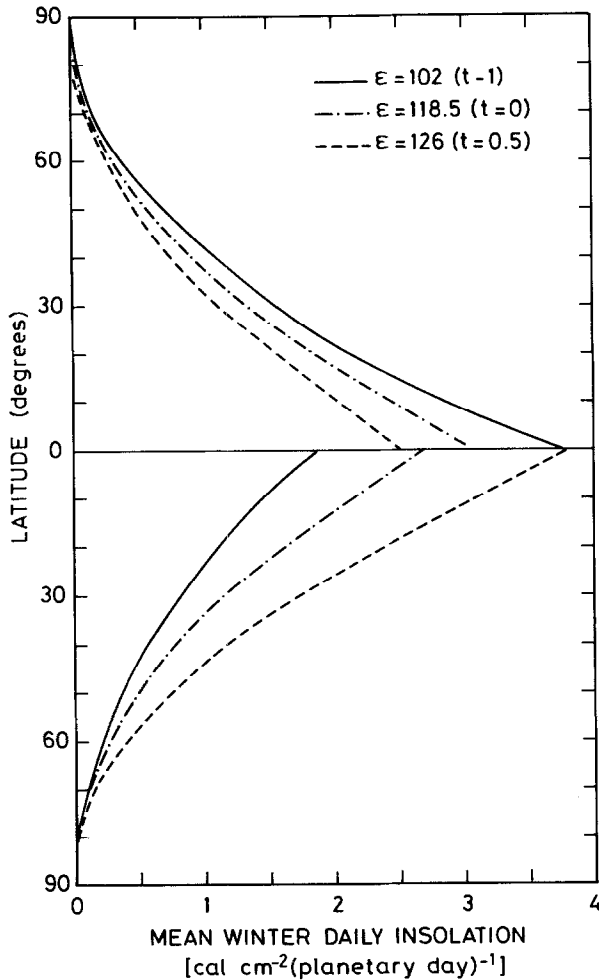


Fig. 7. Latitudinal variation of the mean winter daily insolation ( $\bar{I}_D$ )<sub>W</sub> at the top of the atmosphere of Pluto at  $t = -1$  ( $\epsilon = 102^\circ$ ),  $t = 0$  ( $\epsilon = 118.5^\circ$ ), and  $t = 0.5$  ( $\epsilon = 126^\circ$ )

northern hemisphere and to increase in the southern one. The loss of insolation is of the order of 30%; its gain is nearly twofold. At high latitudes, particularly in the neighborhood of the poles, the obliquity effect is of decreasing significance. The north-south seasonal asymmetry in the distribution of the incident solar flux can also be seen from Figure 7.

For the sake of completeness, the latitudinal variation of the mean annual daily insolation is given in Figure 8. As already stated previously,  $(\bar{I}_D)_A$  can be computed by integrating numerically relation (1) within the appropriate time span of one tropical year. It is, however, expedient to calculate the average yearly insolation by the expression:

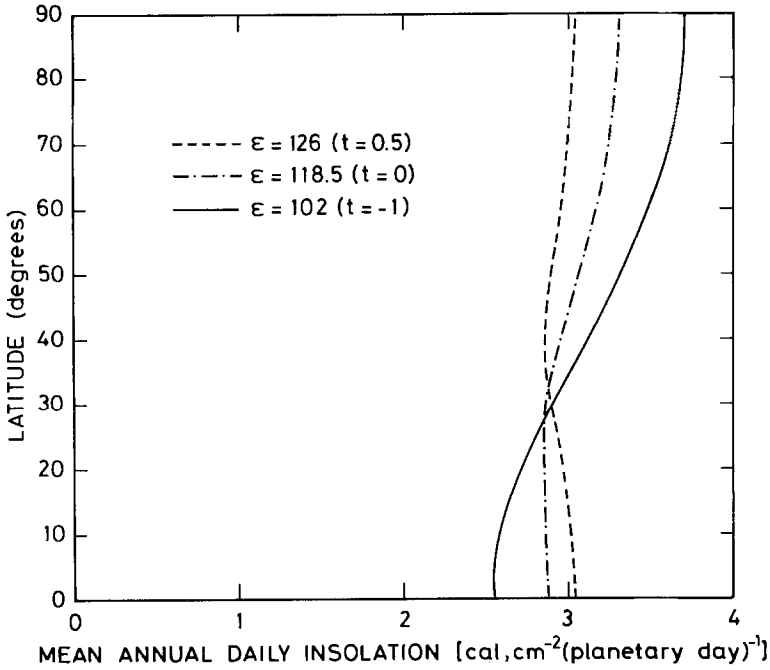


Fig. 8. Latitudinal variation of the mean annual daily insolation  $(\bar{I}_D)_A$  at the top of the atmosphere of Pluto at  $t = -1$  ( $\epsilon = 102^\circ$ ),  $t = 0$  ( $\epsilon = 118.5^\circ$ ), and  $t = 0.5$  ( $\epsilon = 126^\circ$ ).

$$(\bar{I}_D)_A = [(\bar{I}_D)_S T_S + (\bar{I}_D)_W T_W] / T_0 . \quad (17)$$

Taking into account the numerical values of the lengths of the seasons and the tropical year, we find that relation (17) can, in a very good approximation, be written

$$(\bar{I}_D)_A = 0.66 (\bar{I}_D)_S + 0.34 (\bar{I}_D)_W , \quad (\epsilon = 102^\circ) \quad (18)$$

$$(\bar{I}_D)_A = 0.53 (\bar{I}_D)_S + 0.47 (\bar{I}_D)_W , \quad (\epsilon = 118.5^\circ) \quad (19)$$

$$(\bar{I}_D)_A = 0.40 (\bar{I}_D)_S + 0.60 (\bar{I}_D)_W . \quad (\epsilon = 126^\circ) \quad (20)$$

These relationships are valid only for the northern hemisphere; for the southern hemisphere, the constant values in each individual expression have to be reversed.

First, it should be emphasized that for  $54^\circ < \epsilon < 126^\circ$  (Ward, 1974; Vorob'yev and Monin, 1975; Toon *et al.*, 1980) the poles of the outer planets receive more annual average energy than does the equator. Hence, this situation is not only realised by Uranus, but also by Pluto at  $t = -1$  ( $\epsilon = 102^\circ$ ) and  $t = 0$  ( $\epsilon = 118.5^\circ$ ). Past of the critical obliquity of  $126^\circ$  ( $t = 0.5$ ) we have  $(\bar{I}_D)_{A_E} > (\bar{I}_D)_{A_P}$ . This interesting phenomenon is particularly evident from Figure 8 where it can also be seen that the steady decrease in polar insolation  $[(\bar{I}_D)_{A_P} = 3.7, 3.3$  and  $3.1]$  is accompanied by a corresponding increase in the equatorial insolation  $[(\bar{I}_D)_{A_E} = 2.6, 2.9$  and  $3.1]$ . In other words, for  $\epsilon = 102$  and  $118.5^\circ$ , the

decrease amounts respectively to about 30 and 15%; at  $\epsilon = 126^\circ$ , the polar average insolation equals the equatorial one and the maximum difference as a function of latitude is barely 6%.

Secondly, from Figures 1, 2, and 3 and particularly from Figure 5, it follows that the daily insolation at the south pole during summer solstice [ $(I_D)_{SP(ss)} = 20.7$  and  $12.7$  for  $\epsilon = 102$  and  $118.5$  respectively] is appreciably higher than that of the north pole at its summer solstice [ $(I_D)_{NP(ss)} = 7.3$  and  $10.4$ ]. On the other hand, the expression (see e.g. Murray *et al.*, 1973, Ward, 1974, Vorob'yev and Monin, 1975; Van Hemelrijck, 1982b)

$$(\bar{I}_D)_{AP} = S_0 T \sin \epsilon / \pi (1 - e^2)^{1/2} a_\oplus^2, \quad (21)$$

yields a mean annual daily insolation which is the same. This can easily be explained by observing (Table I) that the length of the northern summer (59864, 48249 for  $\epsilon = 102$  and  $126^\circ$  respectively) is longer than the length of the southern summer (30719, 42334), the ratio of both seasons being equal to 1.95 and 1.14. For  $\epsilon = 126^\circ$ , [ $(\bar{I}_D)_{NP(ss)} = 14.1$  and  $(\bar{I}_D)_{SP(ss)} = 7.5$ ; ratio of the seasons: 0.66] the opposite effect is found. It is evident that the above mentioned insolation imbalance vanishes in the total taken over the year, the curves of Figure 8 being perfectly symmetric with respect to the equator.

Finally, Figure 8 clearly indicates that at a latitude of nearly  $30^\circ$ , the mean annual daily insulations are practically constant, the maximum difference attaining scarcely 1.5% at the above mentioned latitude. For latitudes between the equator and  $30^\circ$ , it is found that  $(\bar{I}_D)_A$  ( $\epsilon = 126^\circ$ )  $>$   $(\bar{I}_D)_A$  ( $\epsilon = 118.5^\circ$ )  $>$   $(\bar{I}_D)_A$  ( $\epsilon = 102^\circ$ ); beyond  $30^\circ$ , the inequalities have to be reversed.

## 5. Summary

In this paper, we have presented the insolation at Pluto backward ( $t = -1$ ) and forward ( $t = 0.5$ ) from the present-day epoch and also near the current one ( $t = 0$ ). Two epochs in the past and in the future correspond respectively to a minimum and a maximum value of the long-term motion of the obliquity. The other orbital elements, ( $e$  and  $\lambda_p$ ), which influence the solar radiation and which are also sensitive to periodic variations, were calculated for the time periods in question. As a consequence, the results illustrate the combined effect of the evolving dynamic parameters on the insolation regime of the planet. Although the behaviour of the solar radiation distributions follows in the expected way from the changes in Pluto's eccentricity, obliquity and longitude of the perihelion, the comparison of the solar energy incident at the top of the planet at the three specific epochs reveals some interesting features which may be summarized as follows:

(a) Over the time period of about 1.5 million years, i.e. from  $t = -1$  to  $t = 0.5$ , the maximum solar radiation at the north pole near summer solstice enhances with a factor of about 2, whereas at the south pole this insolation reduces over more than 100%. Whether or not  $(I_D)_{NP(ss)}$  is greater or smaller than  $(I_D)_{SP(ss)}$  is exclusively dependent on the position of the perihelion.

(b) in the obliquity range (102-126°) it is found that the polar summer solstice insolation always exceeds the equatorial one. The ratio of both insulations depends only on the value of  $\epsilon$  and amounts to about 14.8, 5.8, and 4.3 for  $t = -1, 0$  and  $0.5$  respectively.

(c) In going from  $t = -1$  to  $t = 0.5$ , the calculations reveal that the steady increase of  $(I_D)_{NP(ss)}$  is accompanied by a corresponding loss of  $(I_D)_{SP(ss)}$ . Those solar radiations are strongly dependent on  $\epsilon$  and particularly on  $\lambda_p$ , but are only a weak function of the eccentricity.

(d) Over practically the entire solar longitude interval or more precisely for  $20^\circ < \lambda_\odot < 160^\circ$  and  $200^\circ < \lambda_\odot < 340^\circ$ , the solar energies received at the poles are higher than those obtained at the equator.

(e) The shift between the position of maximum solar radiation and the position of summer solstices is owing to the non-coincidence of the latter with the perihelion passage and may reach values of about  $30^\circ$ .

(f) In general, and for eccentric orbits, the daily insolation is strongly affected by the time of the perihelion passage which may create remarkable hemispherical seasonal assymetries in the solar radiation distribution. This is obviously the case for the two epochs forward and backward from the present one. At  $t = 0$ , however, the north-south solar energy distributions are nearly symmetrical due to the fact that the perihelion occurs close to the equinox.

(g) Summer and winter are, roughly speaking, repeated twice a year although this phenomenon is less striking for  $t = 0$  and  $0.5$  than for  $t = -1$ .

(h) From  $t = -1$  to  $t = 0.5$ , the mean summertime insolation in the northern hemisphere increases at all latitudes, maximally by about 100% at the equator; in the southern hemisphere the insolation pattern switches roles with a maximum decrease at the south pole of the order of 50%. The solar radiations are only weakly dependent on changes in  $e$ , but are quite sensitive to fluctuations in both  $\epsilon$  and  $T_s$ .

(i) The loss of the mean winter daily insolation over the time span of  $1.5 \times 10^6$  yr is approximately 30% at all latitudes in the northern hemisphere except at polar region latitudes. In the southern hemisphere, the mean wintertime insolation experiences a nearly twofold increase over the entire latitude interval between the two extremes of the time range used.

(j) The mean annual daily insolation at the poles declines if  $t$  goes from  $-1$  to  $0.5$ ; conversely, the equatorial energy deposition increases. The percent differences are all of the order of 20%. The critical latitude past which the yearly average insolation at  $t = -1$  exceeds that at  $t = 0.5$  is situated near  $30^\circ$ .

(k) At  $t = 0.5$ , which corresponds roughly with an obliquity of  $126^\circ$ , the poles receive as much annual energy than the equator. For the two other epochs,  $(\bar{I}_D)_{AP} > (\bar{I}_D)_{AE}$ .

In conclusion, the calculations presented in this paper, clearly demonstrate how the insolation on Pluto might considerably differ between the present-day epoch orbital configuration and alternatives in the past or in the future. Such changes in the solar energy deposition would have important impact on the climatic history of the planet.

### Acknowledgments

We would like to thank J. Schmitz and F. Vandreck for the realisation of the illustrations. We are also grateful to M. De Clercq for typing the manuscript.

### References

- Brinkman, A. W. and McGregor, J.: 1979, *Icarus* **38**, 479.
- Davies, M. E., Abalakin, V. K., Cross, C. A., Duncombe, R. L., Masursky, H., Morando, B., Owen, T. C., Seidelmann, P. K., Sinclair, A. T., Wilkins, G. A., and Tjufin, Y. S.: 1980, *Celes. Mech.* **22**, 205.
- Dobrovolskis, A. R. and Harris, A. W.: 1983, *Icarus* **55**, 231.
- Golitsyn, G. S.: 1979, *Icarus* **38**, 331.
- Harris, A. W. and Ward, W. R.: 1982, *Ann. Rev. Earth Planet. Sci.* **10**, 61.
- Levine, J. S., Kraemer, D. R., and Kuhn, W. R.: 1977, *Icarus* **31**, 136.
- Murray, B. C., Ward, W. R., and Yeung, S. C.: 1973, *Science* **180**, 638.
- Toon, O. B., Pollack, J. B., Ward, W. R., Burns, J. A., and Bilski, K.: 1980, *Icarus* **44**, 552.
- Van Hemelrijck, E.: 1982a, *Icarus* **52**, 560.
- Van Hemelrijck, E.: 1982b, *Bull. Acad. R. Belg., Cl. Sci.* **68**, 675.
- Van Hemelrijck, E.: 1982c, *Icarus* **51**, 39.
- Van Hemelrijck, E.: 1983, *The Moon and the Planets* **28**, 125.
- Vorob'yev, V. I. and Monin, A. S.: 1975, *Atmos, Ocean. Phys.* **11**, 557.
- Ward, W. R.: 1974, *J. Geophys. Res.* **79**, 3375.
- Williams, J. G. and Benson, G. S.: 1971, *Astron. J.*, **76**, 167.
- Wilson, R. C.: 1982, *J. Geophys. Res.* **87**, 4319.